JLAB-TN-18-003
Rev. June 15, 2018

Magnetic Flux Generated by Thermal Current in CEBAF 5-Cell Cavity System

Shichun Huang*, Rongli Geng

The unloaded quality factor Q_0 of many 5-cell CEBAF cavities was lowered by a factor of ~2 from their vertical qualification testing to their beam operation in CEBAF tunnel. Causes of this Q_0 degradation were studied previously, including a more rent one addressing static fluxes arising from magnetic components near a 5-cell cavity. This note reports on a preliminary study of the dynamic fluxes generated by a thermal current. Such a thermal current arises from the Seebeck effect and flows in closed loops formed by a niobium cavity and its surrounding tuner rods that are made of stainless-steel. The behaviors of magnetic fluxes in response to various thermal profiles on a 5-cell CEBAF cavity with integrated tuner rods were studied in a JLAB VTA dewar. An outcome of this study is a proposed cool-down procedure for eliminating the thermal current generated magnetic fluxes around 5-cell cavities placed in CEBAF tunnels. This procedure may be useful to improve cavity Q_0 in a cost-effective manner, which in turn save cryogenic expenditures for sustaining CEBAF operation.

Introduction

The unloaded quality factor of an RF cavity Q_0 can be described by $Q_0 = {}^{G}/_{R_s}$, where G is the geometry factor determined solely by the cavity geometry, Rs is the RF surface resistance which is consisted of the BCS term R_{BCS} and residual term R_{res}. The Q_0 values of many 5-cell cavities placed in the CEBAF tunnel were degraded by a factor of ~2 as compared to that measured during their vertical qualification testing. The origin of this Q_0 degradation is attributed to an increase of R_{res}. Magnetic fluxes trapped in the RF penetration layer of a SRF cavity during its cool down crossing Tc contribute to R_{res}, as has been well established. Sources of magnetic fluxes include *static* ones, such as the earth magnetic field attenuated by the magnetic shielding, magnetized components enclosed in magnetic shields, and *dynamic* ones such as thermal current generated magnetic fluxes. Prior work revealed large remnant magnetic fields in various magnetic components being near a cavity yet being enclosed inside the inner magnetic shield. That effort led to proscription and partial implementation of mitigation solutions against identified sources of static magnetic fluxes in original CEBAF cryomodules [1].

When a temperature gradient is established in a conductor, an electrical potential difference arises between its ends that are at different temperatures. This is described as the Seebeck effect and the ratio between potential difference developed and the temperature difference is called the Seebeck coefficient (S). S depends on material, temperature, crystal structure and impurities etc. By convention, the sign of S represents the potential of the cold side with respect to the hot side [2]

$$S = \frac{V_c - V_h}{T_h - T_c} = \frac{dV}{dT} \tag{1}$$

Fig. 1 illustrates the CEBAF 5-cell cavity system consisted of a 5-cell niobium cavity and its tuner components including three stainless-steel supporting rods. When a temperature gradient is established over the length of the cavity during the cryomodule cool-down process, a thermal electric current develops due to the Seebeck effect and flows in the closed loops formed by the cavity and the rods. This thermal current will in turn generate magnetic fluxes which may be trapped on the RF surface of the cavity when it enters into the superconducting state.

* Former IMP, CAS graduate student visiting JLab for Ph.D thesis research

The main focus of this work is to experimentally evaluate the thermally generated magnetic fluxes. We carry out measurements of magnetic fluxes in response to various thermal profiles by cooling down or warming up a 5-cell cavity vertically orientated in a VTA dewar. In addition, we seek possible ways to eliminate the thermally generated fluxes. Such techniques may be practically used for elimination of Q_0 degradation from the trapped fluxes arising from the thermal current generated fluxes.

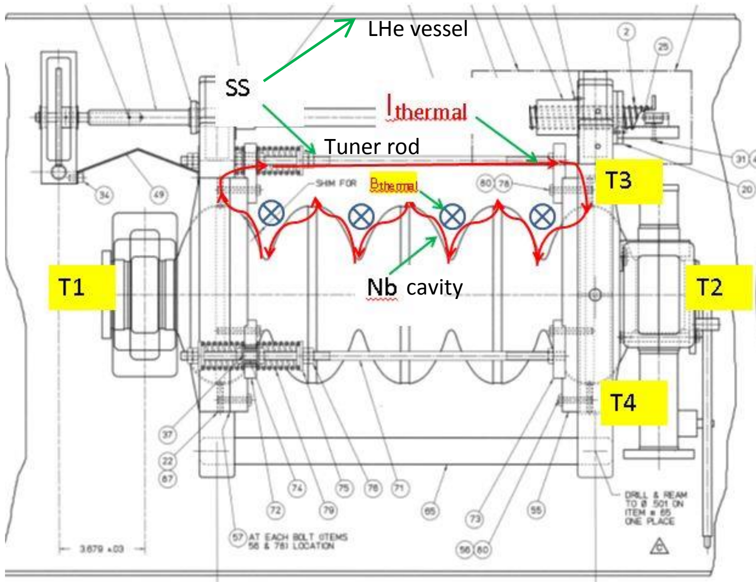

Fig. 1 CEBAF 5-ell cavity system with mounted tuner components. A closed loop is formed by the niobium cavity and stainless-steel tuner rods. A thermal current is resulted when cavity ends are at different temperatures and it flows in this loop. Magnetic fluxes generated by the thermal currents may be trapped in the RF penetration layer of the cavity when it is cooled through the transition temperature of niobium. The stainless-steel liquid helium vessel is also shown.

Measurement Apparatus

We measured the temperature and magnetic flux density at various locations of the outer surface of a 5-cell CEBAF cavity as well as one or three stainless-steel tuner rod while this system was being cooled down or warmed up. All the cavity ports were left open. The arrangement of sensors is schematically shown in Fig. 2 and a detailed description is given in next section. Four Bartington fluxgate magnetometers were attached at selected locations. Two Cernox temperature sensors (CX-1010-SD-1.4L) attached at the upper and lower ends of the rod monitor temperatures TA and TB at these locations. Five silicon diode sensors (XDT-670A-DI-184) attached to the cavity outer surface at different height monitor temperatures at these locations, permitting observation of the thermal path during cool-down or warm-up processes. Each magnetometer attached to the cavity outer surface is accompanied by a silicon diode temperature sensor. This sensor arrangement allows detection of the moment of phase transition between normal and superconducting in these cavity regions.

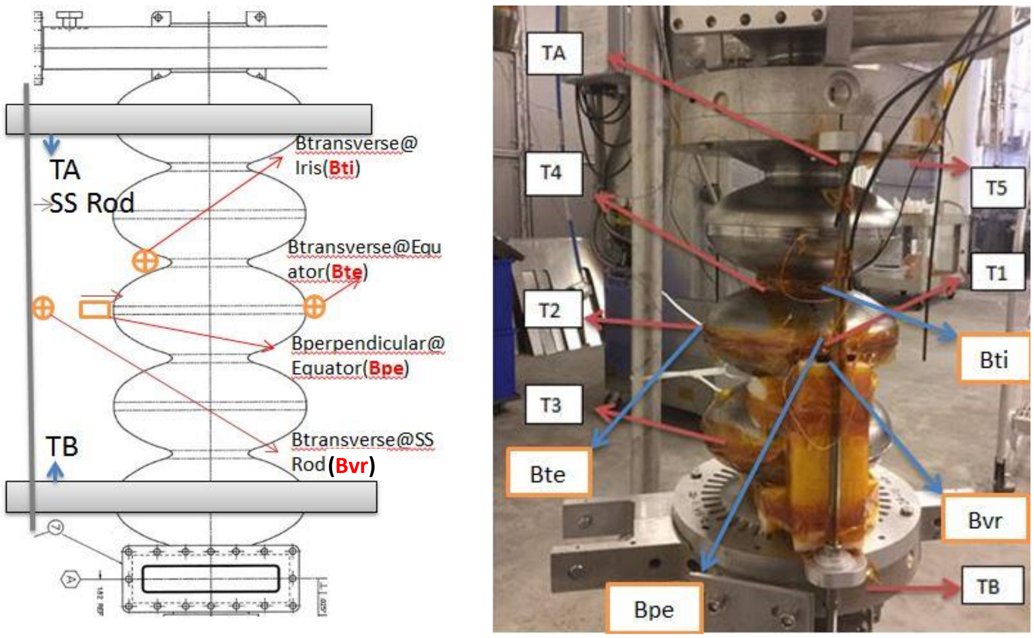

Fig. 2 The testing setup consisting of a CEBAF 5-cell niobium cavity and one stainless-steel tuner rod. Four fluxgate magnetometer sensors are attached to various locations at the cavity and the rod. Two Cernox temperature sensors are attached to the ends of the rod. Additional diode temperatures sensors are attached to the cavity. See text for more details.

Experimental Observations

Thermal Current

The first experimental testing was carried out with a 5-cell CEBAF cavity with an integrated stainless-steel rod vertically orientated in VTA dewar#7. As shown in Fig. 2, four Bartington fluxgate magnetometers were attached at the following locations with the indicated orientation:

- The mid-point of the stainless-steel rod with the sensor axis being perpendicular to the rod axis, providing a sensitive measurement of the magnetic flux generated by a thermal current flowing along the axial direction in the stainless-steel rod (denoted as **Bvr**).
- The side facing toward the rod of the 4th iris with the sensor's cylindrical wall being tangential to the iris OD, providing a sensitive measurement of the transversal magnetic flux at that sensor location (denoted as **Bti**).
- The side facing toward the rod of the 3rd cell equator with the sensor's axis being aligned in the radial direction of the equator OD, providing a sensitive measurement of the magnetic flux component perpendicular to the local surface at that sensor location (denoted as **Bpe**).
- The side facing away from the rod of the 3rd cell equator with the sensor's cylindrical wall being tangential to the equator OD, providing a sensitive measurement of the transversal magnetic flux at that sensor location (denoted as **Bte**).

The measurement results are shown in Fig. 3 – 6. **DeltaT** is defined as the temperature difference between the two ends of the stainless-steel rod (**DeltaT** = TA - TB). In each VTA dewar, the cold helium gas was supplied through a tube reaching the bottom of the dewar. The delivered cold helium gas cooled the testing setup convectively as it moved upward. The spent warm helium gas returned to the refrigeration system via an exit port at the top of the dewar. As a natural consequence, the bottom end of the testing setup was always colder than the top end, hence **DeltaT** > 0, at a given instant during cool-down.

For a cool-down process started at room temperature in equilibrium, **DeltaT** = 0 initially. It then rose and fell as the cool-down proceeded and ultimately would return to 0 again when the testing setup became in equilibrium at 4K.

Fluxes generated by thermal currents were observed over broad range of cavity temperatures. However, fluxes generated by thermal currents when the entire cavity still being in normal conducting state are of no interest to us; fluxes generated after the entire cavity having entered into superconducting state are of no interest either as those fluxes are completely excluded from the superconducting cavity wall (Meissner effect). Of interest to us are those generated over the period starting at the moment of the cavity bottom end becoming superconducting up to the moment of the cavity top becoming superconducting. Only these fluxes might become trapped in the cavity wall (then causing increased RF losses), due to incomplete Meissner effect while the boarder of the normal conducting phase and the superconducting phase being swept upward through the cavity length. For this reason, our data analysis on the thermal current generated flux as shown in Fig. 3-6 are focused for the regime where TB < 10 K.

By turning on a heater located at the bottom of the dewar, any liquid helium collected in the dewar would be evaporated and the testing setup would warm-up from 4K to an intermediate temperature (say 35K). At that point, warm helium gas was injected through a tube with its open end at the bottom of the dewar and this would accelerate the warm-up process. It was found from experiments that the temperature of the testing setup was quite uniform from its bottom to its top during a warm-up process. If the cool-down was re-started while the testing setup was in the process of warm-up to an intermediate temperature, **DeltaT** was typically limited to a small value. We took advantage of this feature for realizing a drastically different **DeltaT** as compared to that achieved in cool-down cycles started at room temperature.

At each sensor location, a background magnetic flux density was registered before cool-down was started while the entire setup was in equilibrium at room temperature. This background was subtracted from the measured flux density during cool-down. Therefore the reported values in these figures are attributed to magnetic fluxes generated by a thermal current. It should be noted that this background field may experience slow drift when the passive magnetic shielding sheet wrapped around the OD of the dewar vacuum vessel was sufficiently chilled due to the small conductive heat leak in the dewar. This effect was monitored during our testing to ensure the background fluxes were correctly subtracted.

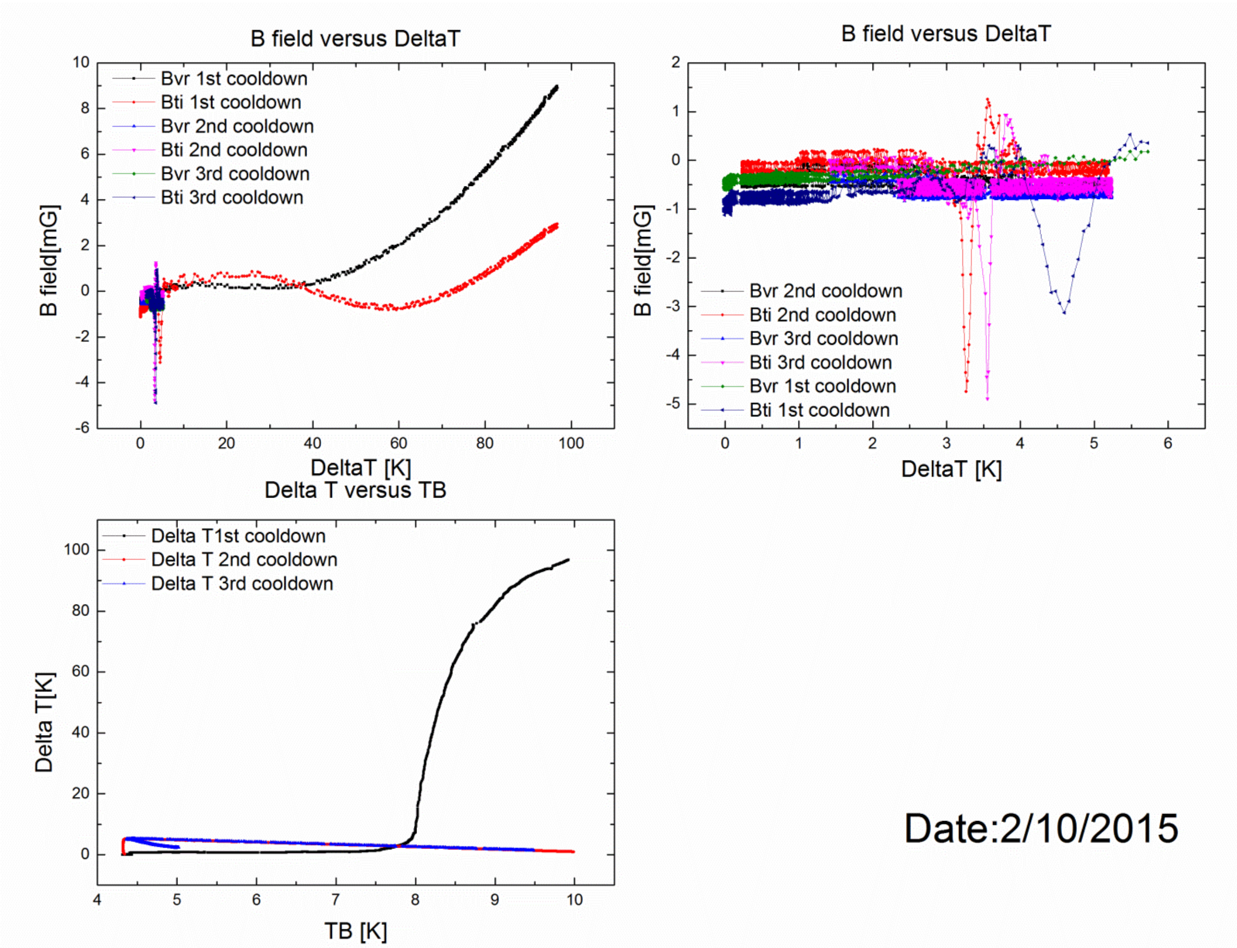

Fig. 3 Measurement results on **Bvr** and **Bti** and their correlation with **DeltaT** from three cool-down cycles on February 10, 2015 (upper left). Thermal current generated magnetic fluxes are evident from both sensors located both at the rod (**Bvr**) and at the 4^{th} iris (**Bti**) for **DeltaT** in the range of 40-100 K during the 1^{st} cool-down after the cavity started to enter into superconducting state from its bottom flange. No significant fluxes were detectable for small **DeltaT** values of < 6K realized during the 2^{nd} and 3^{rd} cool-down cycles. Details for **DeltaT** in the range of 0-6K reveal impulsive responses in **Bti** (upper right) which will be discussed later. Correlation between **DeltaT** and **TB** is shown in the lower graph. The first cool-down began at room temperature, resulting a large temperature difference between the two ends of the cavity/rod system. The 2^{nd} and 3^{rd} cool-down cycles were carried out after the system was warmed up to an intermediate temperature following initial cool-down to 4 K.

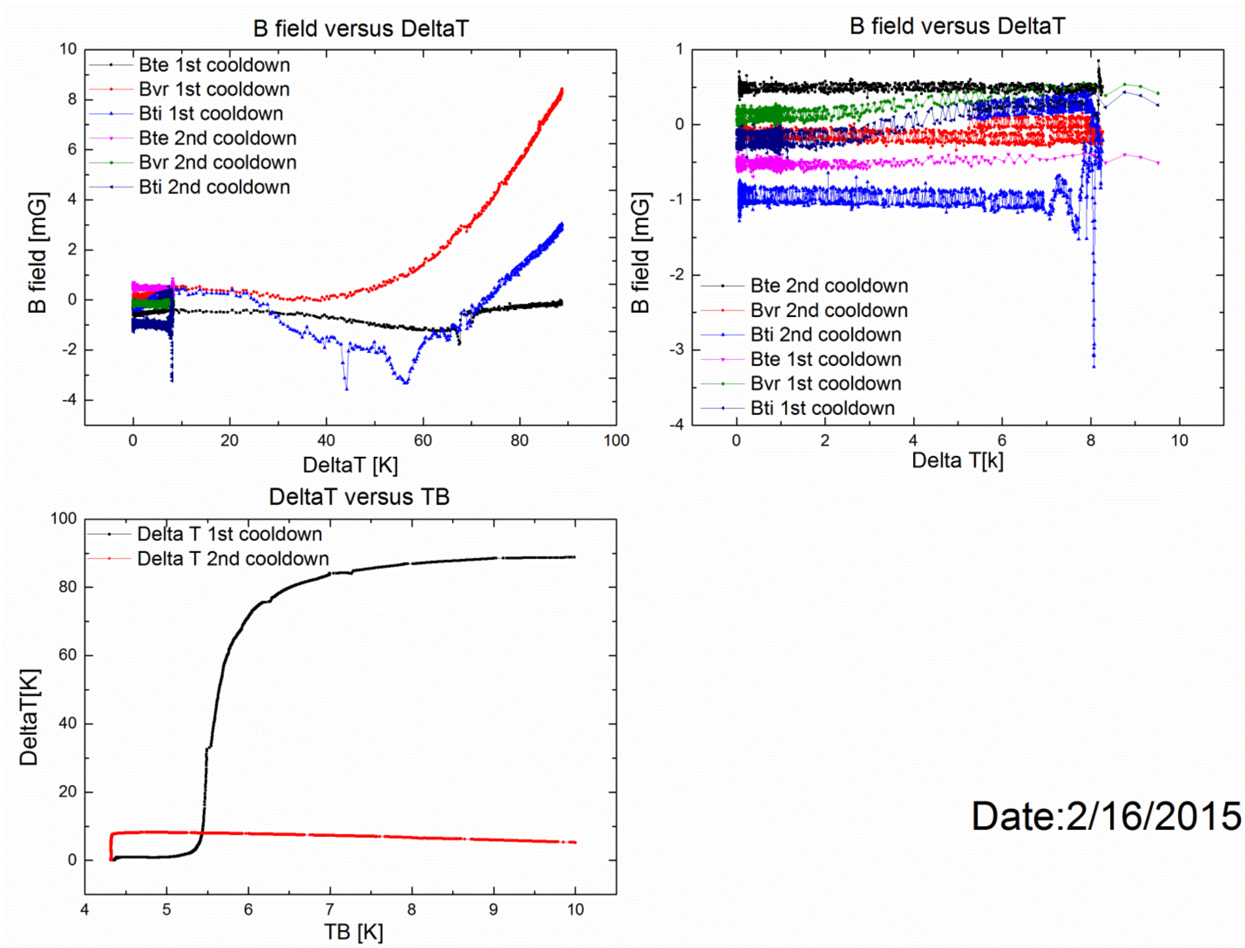

Fig. 4 Measurement results on **Bte**, **Bvr** and **Bti** and their correlation with **DeltaT** from two cool-down cycles on February 16, 2015 (upper left). Thermal current generated magnetic fluxes are evident from three sensors located and at the 3rd equator (**Bte**), at the rod (**Bvr**), and at the 4th iris (**Bti**) for **DeltaT** in the range of 30-90 K during the 1st cool-down after the cavity started to enter into superconducting state from its bottom flange. No significant fluxes were detectable for small **DeltaT** values of < 6K realized during the 2nd cool-down cycle. Details for **DeltaT** in the range of 0-9K reveal impulsive responses in **Bti** (upper right) which will be discussed later. Correlation between **DeltaT** and **TB** is shown in the lower graph. The first cool-down began at room temperature, resulting a large temperature difference between the two ends of the cavity/rod system. The second cool-down was carried out after the system was warmed up to an intermediate temperature following initial cool-down to 4 K.

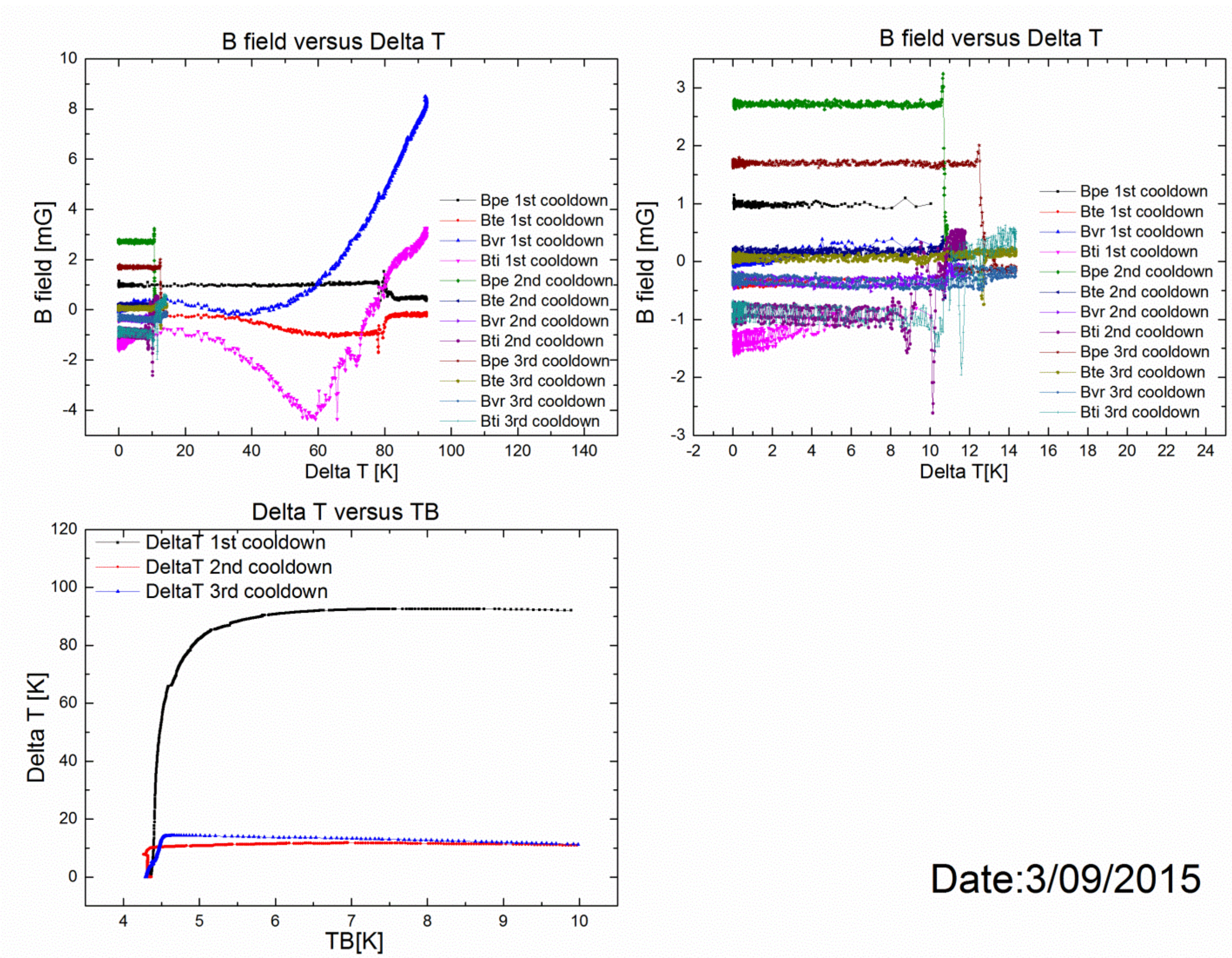

Fig. 5 Measurement results on **Bpe**, **Bte**, **Bvr** and **Bti** and their correlation with **DeltaT** from three cool-down cycles on March 9, 2015 (upper left). Thermal current generated magnetic fluxes are evident from four sensors located and at the 3rd equator (**Bpe** and **Bte**), at the rod (**Bvr**), and at the 4th iris (**Bti**) for **DeltaT** in the range of 30-90 K during the 1st cool-down after the cavity started to enter into superconducting state from its bottom flange. No significant fluxes were detectable for small **DeltaT** values of < 15K realized during the 2nd and 3rd cool-down cycles. Details for **DeltaT** in the range of 0-7K reveal impulsive responses in **Bpe** and **Bti** (upper right) which will be discussed later. Correlation between **DeltaT** and **TB** is shown in the lower graph. The first cool-down began at room temperature, resulting a large temperature difference between the two ends of the cavity/rod system. The 2nd and 3rd cool-down cycles were carried out after the system was warmed up to an intermediate temperature following initial cool-down to 4 K.

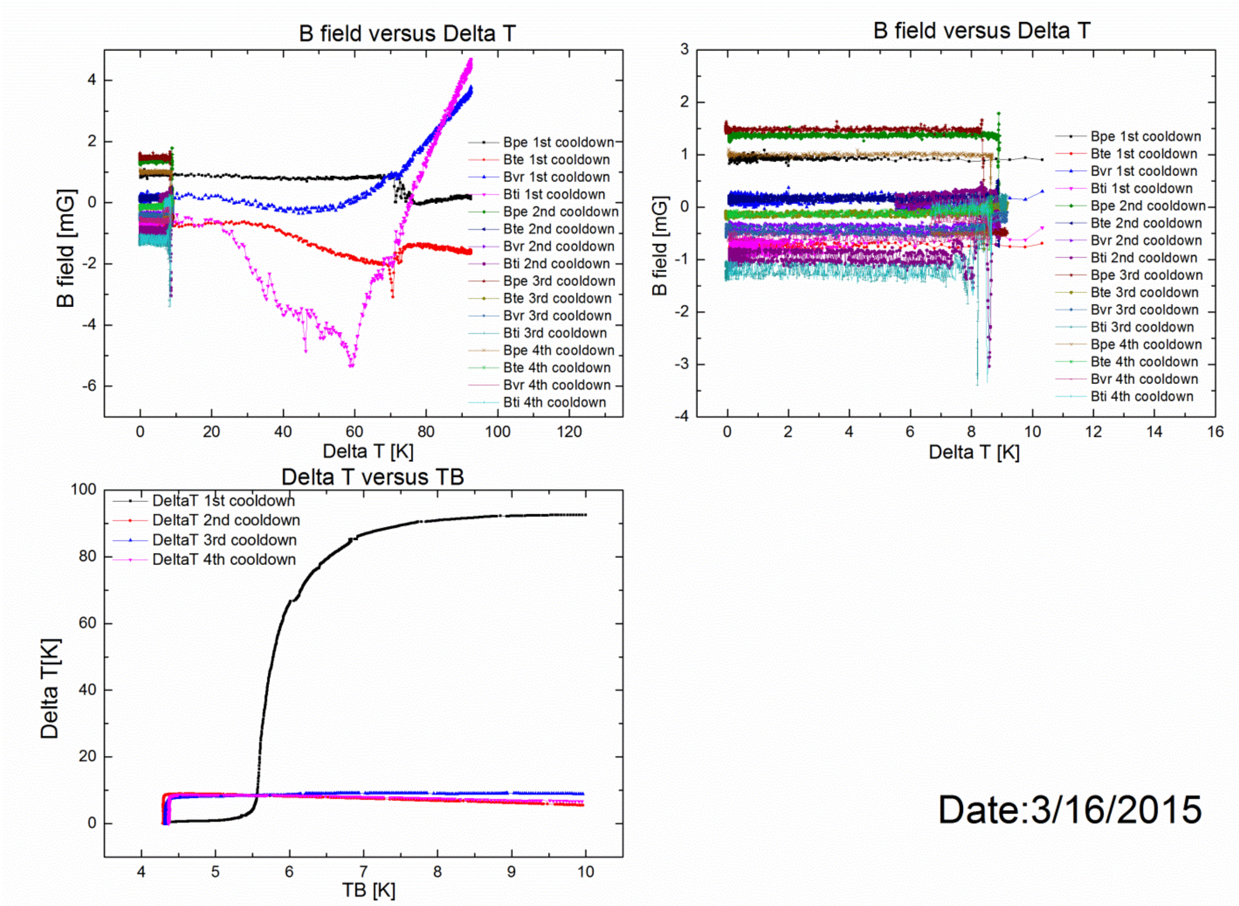

Fig. 6 Measurement results on **Bpe**, **Bte**, **Bvr** and **Bti** and their correlation with **DeltaT** from four cool-down cycles on March 16, 2015 (upper left). Thermal current generated magnetic fluxes are evident from four sensors located and at the 3rd equator (**Bpe** and **Bte**), at the rod (**Bvr**), and at the 4th iris (**Bti**) for **DeltaT** in the range of 20-90 K during the 1st cool-down after the cavity started to enter into superconducting state from its bottom flange. No significant fluxes were detectable for small **DeltaT** values of < 10 K realized during the 2nd – 4th cool-down cycles. Details for **DeltaT** in the range of 0-9 K reveal impulsive responses in **Bpe** and **Bti** (upper right) which will be discussed later. Correlation between **DeltaT** and **TB** is shown in the lower graph. The first cool-down began at room temperature, resulting a large temperature difference between the two ends of the cavity/rod system. The 2nd – 4th cool-down cycles were carried out after the system was warmed up to an intermediate temperature following initial cool-down to 4 K.

Several observations and conclusions can be made from the results shown in Fig. 3-6:

- Magnetic fluxes correlated with the temperature difference between the two ends of the cavity are detected near the cavity outer surface at equator and iris locations as well as near the stainless-steel rod, confirming the existence of thermal current in the closed-loop formed between the CEBAF 5-cell niobium cavity and its stainless-steel tuner components when the two ends of the cavity are at different temperatures.

- The testing setup includes a 5-cell niobium cavity and one stainless-steel rod, permitting sensitive detection of the total thermal current by the flux gate magnetometer attached to the mid-point of the rod. The flux density detected by this sensor (**Bvr**) bottoms out at a value < 0.5 mG when **DeltaT** becomes < 40 K. This behavior is repeatedly observed. This observation implies that by controlling the temperature difference between the two ends of the 5-cell cavity to < 40 K, the thermal current generated magnetic flux can be essentially eliminated.
- The temperature difference between the two ends of the 5-cell niobium cavity can be controlled to be < 15 K during a second cool-down after warming up the cavity system from 4 K to an intermediate temperature (say 40 K). As warming up a niobium cavity above 9.25 K results in complete release of trapped fluxes, a practical procedure emerges from this observation for reliable elimination of thermal current generated magnetic fluxes in 5-cell cavities installed in CEBAF tunnels:
    - Standard cool down to and equalize cavity temperature at 4 K.
    - Warm up cavity to 40 K.
    - Re-cool-down to 4 K.
- The responses of fluxgate magnetometers attached to the cavity outer surface are more complex as compared to that attached to the stainless-steel rod. This observation seems to indicate that these sensors are detecting not only to the fluxes generated by the thermal current but also the fluxes expelled from the cavity wall due to Meissner effect.

Magnetic Flux Transient at Cavity Surface while Cooling/Warming Across Tc

As mentioned in previous section, the responses of the fluxgate magnetometers attached to the cavity outer surface are more complex. More detailed measurements were therefore carried out by co-locating temperature sensors with flux gate magnetometers. This approach permitted simultaneous tracking of the magnetic flux and the temperature at various locations at the cavity surface. It allowed resolving transient flux expulsion due to Meissner effect while the local surface was cooling/warming across Tc.

Fig. 7 shows magnetic flux densities detected by various magnetometers as a function of the *local* temperature monitored by the co-located diodes for the cool-down and warm-up cycles on March 9, 2015. The testing setup consisted of one 5-cell niobium cavity and one stainless-steel rod for this measurement.

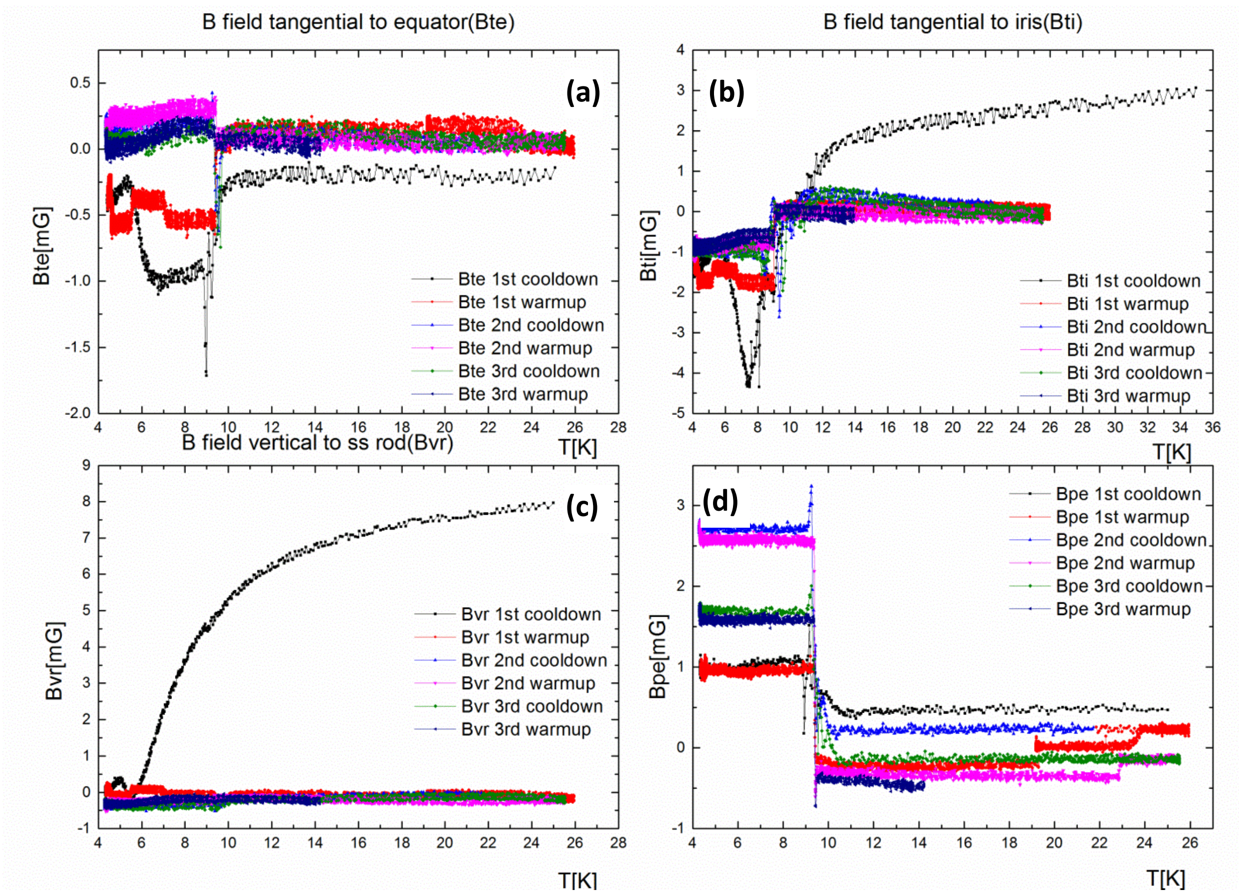

Fig.7 Variation of magnetic flux densities measured at different locations at the cavity outer surface with local temperatures for cool-down warm-up cycles on March 9, 2015.

Several observations can be made from the results shown in Fig. 7:

- A sharp transient is detected by a magnetometer attached to the cavity outer surface when the temperature at the sensor location crosses 9.2-9.3 K. This can be seen in Fig. 7 (a), (b), and (d) which shows the dependence of the detected flux density at each location on the local temperature: (a) **Bte**, for the magnetometer with its cylindrical wall attached to the 3rd cell equator and its axis lying in the equator plane; (b) **Bti**, for the magnetometer with its cylindrical surface attached to the 4th iris and its axis lying in the iris plane; (d) **Bpe**, for the magnetometer with its flat end-surface attached to the 3rd equator and axis lying in the equatorial plane. This transient is best illustrated in Fig. 7(d) which shows a jump-up with large signal-to-noise ratio in **Bpe** on each occasion of cooling down across 9.3 K and a jump-down on subsequent warming up across 9.3 K.
- These observed transients are consistent with the Meissner effect, namely magnetic fluxes are expelled from the cavity wall when the local temperature crosses the transition temperature of niobium Tc = 9.25K. The expelled fluxes cause a flux density increase near the cavity outer surface, therefore a jump-up (jump-down) step in the detected flux density if the initial flux density in the normal conducting state is positive (negative). During the warm-up following each cool-down, the previously expelled fluxes return to the cavity wall instantly when Tc is crossed again, hence a step in the reversed direction as compared to that during cool-down.

- The observed *step transients* in **Bte** near Tc = 9.25 K for the 1st cool-down/warm-up cycle shown in Fig. 7(a) can be explained by the Meissner effect. The apparent non-zero value -0.25 mG above Tc during the first cool-down can be attributed to the effect of magnetic flux generation from thermal currents. For the 2nd and 3rd cool-down/warm-up cycles, despite the difficulty in identifying steps near Tc because of poor signal-to-noise ratio, an impulse is clearly recorded on each occasion of Tc being crossed. In fact, such impulses are observed to accompany the step transient during the first cool down. The reason for those impulses is not understood.
- Step transients in **Bti** are clearly observed on each occasion of Tc being crossed either during cool-down or warm-up. However, **Bti** exhibits a rather sophisticated variation with the local temperature during the 1st cool down while the thermal current generation is most significant: it is positive above Tc and decreases smoothly as the local temperature decreases. It has *crossed zero* and ends up with a negative value when the local temperature reaches Tc. This unusual variation in **Bti** involving zero crossing during the first cool-down started at room temperature is observed rather reliably (see Fig. 3-6), therefore we believe there is a underlying physical reason.
- Both **Bte** and **Bti** exhibit large drifting away from their peak values when the local temperature is well below Tc during the first cool-down. In addition, there are noticeable jump-up and jump-down steps between 4K and 9K during the first warm-up. The reason behind these variations is not understood. In light of the new understanding learned recently [3], one possible reason might be the uncontrolled variation in the VTA environment. Further measurements are needed to allow firm analysis of flux density variation at temperature away from Tc.
- Transient steps in **Bpe** are detected with large signal-to-noise ratios when the local temperature crosses Tc during the repeated cool-down and warm-up cycles (see Fig. 7(d)). This result is unexpected and deserves further analysis.
    1. The **Bpe** values at temperatures above Tc exhibit variations well above the singal noise level from -0.5 to 0.5 mG. In the simple model of a thermal current flowing along the curved path defined by the cavity contour, no thermal current generated flux is expected in the direction of the sensor axis for **Bpe** (namely the normal direction of the cavity outer surface). One possible reason for these non-zero **Bpe** above Tc is the uncontrolled variation in the VTA environment [3].
    2. Putting aside the origin of these varying non-zero values above Tc, one can see that each time the temperature is lowered to cross Tc, **Bpe** jumps upward and then settles at a positive value, which varies from cycle to cycle (as low as 1.0 mG or as high as 2.7 mG). The variation in **Bpe** at T<Tc is apparently larger than that at T> Tc.

What is the reason behind these unexpected transient steps in **Bpe**? There is apparent geometric explanation: expelled vertical fluxes following the cell contour gives rise to flux component in the direction perpendicular to the local cavity surface at T<Tc. Could this effect alone sufficient to account for the observed jump crossing Tc? Are there other contributors? Does it imply that *the fluxoids due to frozen fluxes tend to align themselves so that the flux tubes are always perpendicular to the cavity wall irrespective of the flux line orientation before phase transition?* Future studies in flux expulsion from or trapping in niobium cavity walls should expand the diagnostics to include monitoring of the flux density in that direction (perhaps not only on the outer surface but also the inner surface).

- Lastly, we should mention that a clear signal in **Bvr** was detected during the first cool-down started at room temperature, while a large temperature difference between the ends of the cavity was established. In contrast, **Bvr** approached to a near-zero value during the 2nd and 3rd cool-down cycles, while a vanishingly small temperature difference was achieved by re-start the cooling following a partial warm up from 4K to an intermediate temperature (~ 40K).

Fig. 8 shows magnetic flux densities detected by magnetometers as a function of the local temperature monitored by the co-located diodes for the cool-down and warm-up cycles on March 16, 2015 with three stainless-steel rods. The 3-rod configuration is standard for 5-cell cavities placed in CEBAF tunnels.

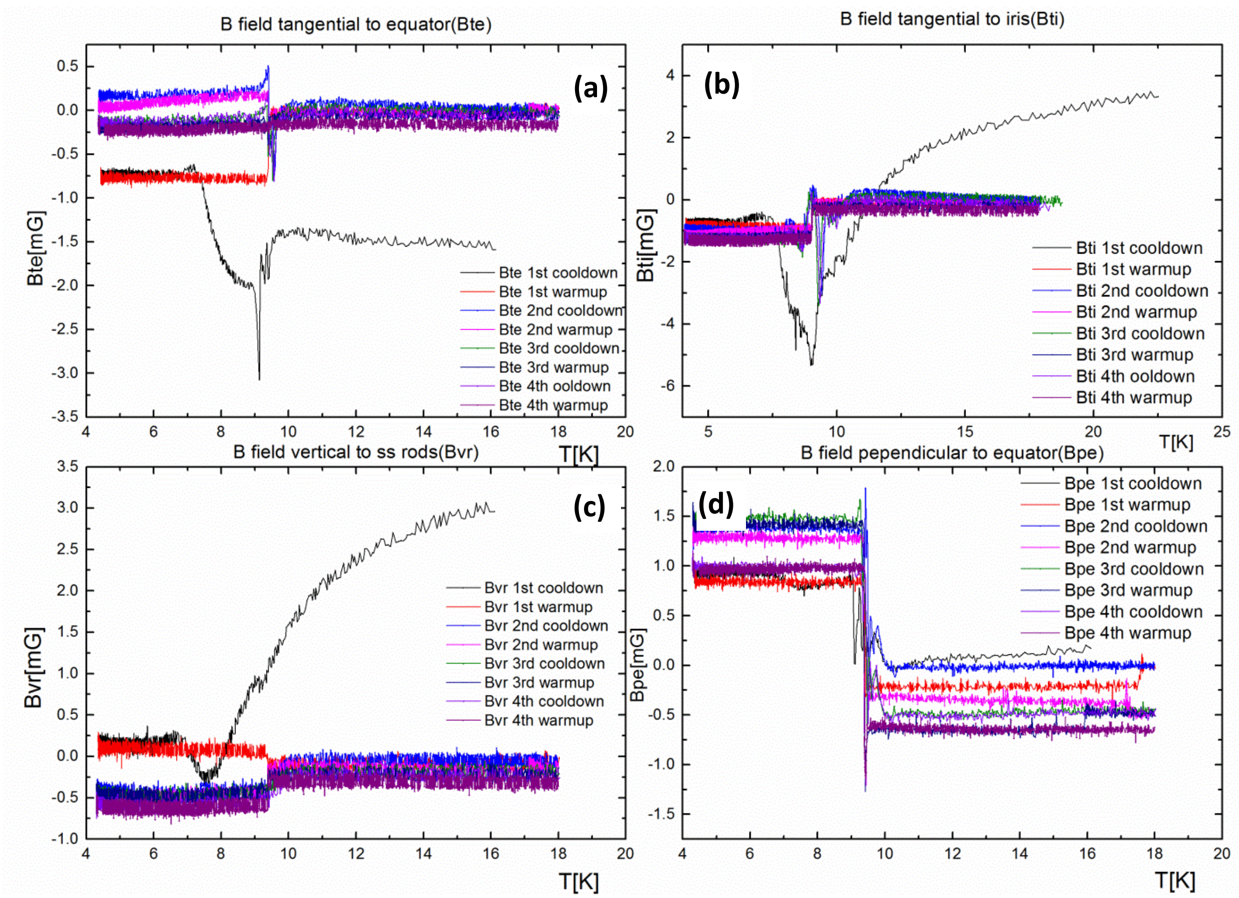

Fig. 8 Variation of magnetic flux densities measured at different locations at the cavity outer surface with local temperatures for cool-down and warm-up cycles on March 16, 2015.

For the 3-rod configuration, similar observations can be made in comparison to that for the 1-rod configuration. An apparent deviation lies in a much smaller **Bvr** and a much larger **Bte** and **Bti**. For example, at 10 K, **Bvr** is 1.5 mG for 3-rod and 5.0 mG for 1-rod; **Bte** is -1.4 mG for 3-rod and -0.3 mG for 1-rod; **Bti** is -2.0 mG for 3-rod and -0.3 mG for 1-rod.

The observed deviation between the 3-rod and 1-rod configuration can be understood as a result of additive effect of currents in multiple rods. It follows then the thermal current passing the cavity may be quite significant with increasing number of rods. The stainless-steel helium vessel hosting the cavity pair in the real CEBAF cryomodule can be regarded as a limiting case with infinite number of rods. Therefore, the actual magnetic flux generated by thermal currents flowing in the wall of a 5-cell cavity placed in a CEBAF tunnel may be might be quite high, due to the combined effects of stainless-steel tuner rods and the liquid helium vessel, if similar temperature difference is established over the ends of a cavity pair.

Summary

We carried out a series of experimental measurements with a 5-cell CEBAF niobium cavity and integrated stainless-steel tuner rod, instrumented with thermometers and magnetometers, for assessment of the *dynamic magnetic fluxes* generated by a thermal current arising from the Seebeck effect. Measurements were done in JLab VTA with the cavity vertically oriented which permitted establishing a temperature difference over the length of the cavity/rod system. This preliminary study confirms the existence of thermal currents flowing in the closed loop formed by the niobium cavity and the stainless-steel tuner rods when a temperature difference of > 40 K is established. This thermal current generated flux increases with the number of rods mounted around the cavity. Based on this observation, we speculate that a significant thermal current may exist arising from the presence of stainless-steel helium vessel, in addition to the tuner rods, around the cavity pair in a real cryomodule placed in CEBAF. *A cool down procedure is proposed for elimination of the thermal current generated magnetic fluxes in 5-cell cavities in CEBAF tunnel: after standard initial cool-down to 4 K, warm up cavity to 40 K, then re-cool-down to 4 K followed by pumping down to 2 K.* A test in CEBAF is recommended.

An unexpected result of this study is the observation of a large transient step in the flux density detected at the outer surface of the equator region of the 5-cell cavity in the direction perpendicular to the local surface. This puzzling phenomenon deserves further studies.

The results of this study naturally raise the question about the thermal current generated magnetic fluxes around 7-cell niobium cavities installed in CEBAF for its energy upgrade to 12 GeV. These 7-cell cavities are surrounded by stainless-steel helium vessels as well and similar *dynamic magnetic fluxes* are possible.

This study should be regarded as a first step in understanding the generation of thermal currents in CEBAF cavities due to Seebeck effect. Further studies should follow as a deeper understanding of this phenomenon may lead to better cavity Q_0 or smaller cryogenic expenditures for sustaining CEBAF operation.

References

[1] R.L. Geng et al., in Proceedings of IPAC2014, Dresden, Germany (2014), THOBB01.

[2] S.O. Kasap, Principles of electronic materials and devices. ISBN10: 0078028183 ISBN13: 9780078028182. http://Materials.Usask.Ca

[3] As is well known at the time of the publication of this tech note from extensive recent (2017-2018) flux expulsion measurements carried out with CEBAF 12 GeV upgrade cavities, a flux gate magnetometer attached to a 7-cell cavity parked in dewar 4 is sensitive enough to detect flux density jumps in the range of 0.1 - 6 mG due to changes in surrounding conditions such as control room door opening/closing, overhead crane movement, radiation shielding block movement etc. At the time (2015) of the studies presented in this note, the detector sensitivity to those environmental changes was not known to us therefore no attention was paid to the control of surrounding conditions.